NJC

Accepted Manuscript

This is an *Accepted Manuscript*, which has been through the Royal Society of Chemistry peer review process and has been accepted for publication.

Accepted Manuscripts are published online shortly after acceptance, before technical editing, formatting and proof reading. Using this free service, authors can make their results available to the community, in citable form, before we publish the edited article. We will replace this *Accepted Manuscript* with the edited and formatted *Advance Article* as soon as it is available.

You can find more information about *Accepted Manuscripts* in the Information for Authors.

Please note that technical editing may introduce minor changes to the text and/or graphics, which may alter content. The journal's standard Terms & Conditions and the Ethical guidelines still apply. In no event shall the Royal Society of Chemistry be held responsible for any errors or omissions in this *Accepted Manuscript* or any consequences arising from the use of any information it contains.

ROYAL SOCIETY OF CHEMISTRY

www.rsc.org/njc

Phototransformation-Pattern of Antiplatelet Drug Tirofiban in Aqueous Solution, Relevant to Drug Delivery and Storage.

Théo Henriet[1a], Philippe-Henri Secrétan[1a], Fatma Amrani[1], Hassane Sadou Yaye[1,3], Melisande Bernard[2], Audrey Solgadi[4], Najet Yagoubi[1] and Bernard Do[1,2*]

[1] Université Paris Sud, UFR de Pharmacie, Groupe Matériaux et Santé. 5, rue Jean Baptiste Clément, 92296 Châtenay-Malabry.
[2] Assistance Publique-Hôpitaux de Paris, Agence Générale des Equipements et Produits de Santé, Département de Contrôle Qualité et Développement Analytique, 7 rue du Fer à Moulin, 75005 Paris, France.
[3] Assistance Publique-Hôpitaux de Paris, Groupe Hospitalier Pitié-Salpêtrière, Service de Pharmacie. 47-83 Boulevard de l'Hôpital, 75013 Paris.
[4] Université Paris-Sud, UFR de Pharmacie, SAMM - Service d'Analyse des Médicaments et Métabolites, Institut d'Innovation Thérapeutique. 5, rue Jean Baptiste Clément, 92296 Châtenay-Malabry.
[a] The first 2 authors contributed equally to this study and are therefore considered as first authors.

ABSTRACT: Tirofiban is a synthetic, nonpeptidic fibrinogen receptor antagonist used as antiplatelet drug by intravenous delivery. As the active pharmaceutical ingredient may undergo light exposure during manufacturing, storage and/or delivery, there is a need to acquire an extensive knowledge of its major photochemical-degradation pathways. Thus, photochemical-degradation of tirofiban under simulated light irradiation in aqueous solution and devoid of photosensitizers or photocatalysts, has been investigated in terms of mechanism. The structural characterization of the photochemical products was carried out with high performance liquid chromatography-multistage high-resolution mass spectrometry along with on-line

hydrogen/deuterium exchange. The identification of the twelve-detected photochemical products suggested that the photo-transformation of tirofiban occurred via multiple reaction pathways, initiated either by electron or hydrogen atom transfer. That included the photo-oxidation of the piperidine moiety without impacting the secondary amine, the hydroxylation of the methylene group activated by the aromatic ring, the oxidation of the alkyl-sulfonamide group and also the decarboxylative oxidation of the molecule. Hydroxylated compounds, geminal and vicinal-diol compounds were highlighted, suggesting that most of the photoproducts are more hydrophilic than the drug. Understanding the main photo-degradation routes is a good basis to work out efficient measures so as to mitigate or avoid tirofiban instability.

▪ INTRODUCTION

Tirofiban, is a synthetic, nonpeptidic fibrinogen receptor antagonist[1] (S)-2-(butylsulfonamino)-3-(4-[4-(piperidin-4-yl)butoxy]phenyl)propanoic acid (Fig. 1), currently licenced as an injectable antiplatelet drug. It acts as a competitive ligand of GPIIb/IIIa receptors located on platelets[2], allowing platelet aggregation prevention by inhibition of fibrinogen binding on activated platelets. Tirofiban is prescribed in the treatment of acute coronary syndrome[3-5] or percutaneous coronary intervention procedures[6]. The drug product is delivered by intravenous route, under a recommended protocol consisting of a 5 minutes bolus (25 µg/kg/min), followed by a maintenance infusion (0.15 µg/kg/min), which can last up to 18 hours. The drug product is supplied in the form of a 0.05 mg/mL-premixed solution. The premixed solution bag is protected from light exposure by a secondary opaque packaging. This kind of packaging has been designed to protect drug products from light exposure.

However, misuse or improper drug storage can occur, causing a potential deterioration in initial quality and especially for liquid preparations, usually much more photolabile than solid formulations of the same drug substance. Additionally, it has been reported that photodecomposition can in some cases lead to the formation of minor degradation products responsible for some adverse effects[7] and there is also a growing literature that clearly demonstrates links between photostability and phototoxicity[8-10] or photogenotoxicity[11]. As a result, there is a need to assess the photostability of the drug in details before being able to understand the risks and benefits to the patient.

From a general point of view, photo-reactivity is rather ubiquitous since for photolytic degradation to occur, radiation must be absorbed either by the drug substance, the formulation or the adventitious presence of impurities. A recent literature survey has revealed that tirofiban was shown stable in glass containers for at least 4h when combined with various other drugs[12]. In another published work, it was shown susceptible to light, with rapid degradation when exposed at 282 nm and 308 nm[13], but on the whole, the data inherent in the characterization of photoproducts likely to form are still unavailable. Hence, the goal of this study was to identify various photoproducts and characterize the main photo-degradation pathways of tirofiban in aqueous solution, when exposed to simulated sunlight irradiation.

Liquid chromatography multistage mass spectrometry studies in combination with accurate mass measurements have been increasingly used for structural characterization of degradation products[14-18]. Therefore, structural analysis of

tirofiban's photoproducts was carried out using this approach type, combined with on-line hydrogen/deuterium exchange.

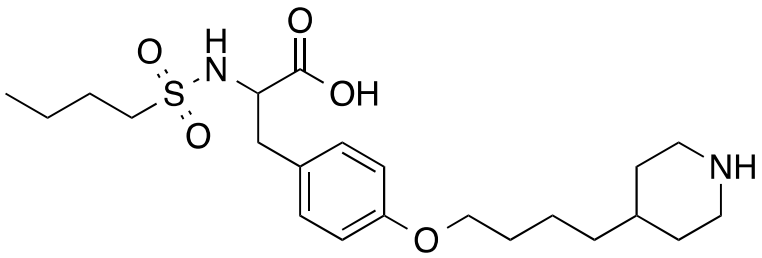

Fig. 1. Chemical structure of tirofiban

▪ EXPERIMENTAL SECTION

MATERIALS. Tirofiban (purity: 98.5%), Deuterated water (D_2O, purity: 99.9%), liquid chromatography(LC)-grade acetonitrile and ammonium formate were purchased from SIGMA-ALDRICH® (St. Louis, USA). Ultrapure water from Q-Pod Milli-Q system (Millipore, Molsheim, France) was used for dissolution, dilution and as a component of the mobile phase.

PHOTOLYSIS EXPERIMENTS. Each experiment was performed in triplicate using 50 µg/mL tirofiban aqueous solutions, allocated in 15 mL hermetically sealed glass vials. A xenon test chamber Q-SUN Xe-1 (Q-Lab Westlake, USA) operating in window mode with a spectrum ranging from 300 to 800 nm, was used for the photolysis studies. The delivered light intensity was of 1.50 W/m² for 24 hours time. Aliquots of samples were withdrawn at various intervals (2, 4, 6, 8, 12, 24 hours) and substrate decay was measured by LC-mass spectrometry (LC-MS^n) in single reaction monitoring mode (441➔276).

ANALYTICAL PROCEDURES. LC was performed using a Dionex Ultimate 3000 system (DIONEX, Ulis, France) consisting of a quaternary pump, a degasser, a thermostated autosampler with a 200 µL-injection syringe and a thermostated column compartment. C18 XTERRA (WATERS, Ireland) 250 mm length, 4.6 mm internal diameter and 5 µm particle size column was used as stationary phase. Mobile phase was composed of A: 10 mM ammonium formate in ultrapure water and B: acetonitrile. The gradient chromatographic program was the following: B 15 % *v/v* from 0 to 2 min; B 15 % to 100 % *v/v* from 2 to 17 min; B 100 % to 15 % *v/v* from 17 to 22 min and 15 % *v/v* from 22 to 25 min. The flow-rate was set at 0.8 mL min^{-1}. LC-high-resolution multistage mass spectrometry (LC-HR-MS^n) was performed by coupling a Dionex® LC system to an electrospray ionisation (ESI)-LTQ-Orbitrap Velos Pro system, composed of a double linear trap and an orbital trap (Thermo Fisher Scientific, CA, USA). Analyses were carried out in positive ion mode with the following conditions: the source voltage and source current were set at 3.4 kV and 100 uA respectively and the temperatures were fixed at 350 °C (source) and 300 °C (capillary). S-Lens was set at 60%. Sheath gas flow and auxiliary gas flow were set at 40 and 20 (arbitrary units), respectively. Acquisition in full scan mode over the mass range of 50-600 Da was used for the detection of the degradation products. High-resolution fragmentation studies were performed using collision induced dissociation mode with the following parameters: minimal signal required: 500, isolation width: 2.00, normalized collision energy: 35.0, default charge state 1, activation Q: 0.250 and activation time 10.0 (arbitrary units). The MS data were processed using Xcalibur® software (version 2.2 SP 1.48). On-line *H/D* exchange(HDX) studies were carried out on each photoproduct by injecting D_2O

during elution of the peak of interest through an additional loop of the MS instrument. Tirofiban absorption spectrum was obtained by the analysis of 50 µg.mL^{-1} tirofiban aqueous solution using a Jasco V550 (Jasco, Maryland, U.S.A) spectrophotometer.

▪ RESULTS AND DISCUSSION

Photostability of 50 µg mL^{-1} tirofiban in aqueous solution was studied over a spectrum range of 300-800 nm. The photoproducts formed were detected and characterized by LC-HR-MS^n and HDX studies.

DEGRADATION OF TIROFIBAN AND DETECTION OF PHOTOPRODUCTS. The UV-visible absorption spectrum of tirofiban in aqueous solution shows abundant absorption from 200 to 350 nm, with a characteristic band at 226 nm and a shoulder at 278 nm (Fig. 2). Absorption above 290 nm suggests that the active substance could degrade under solar light.

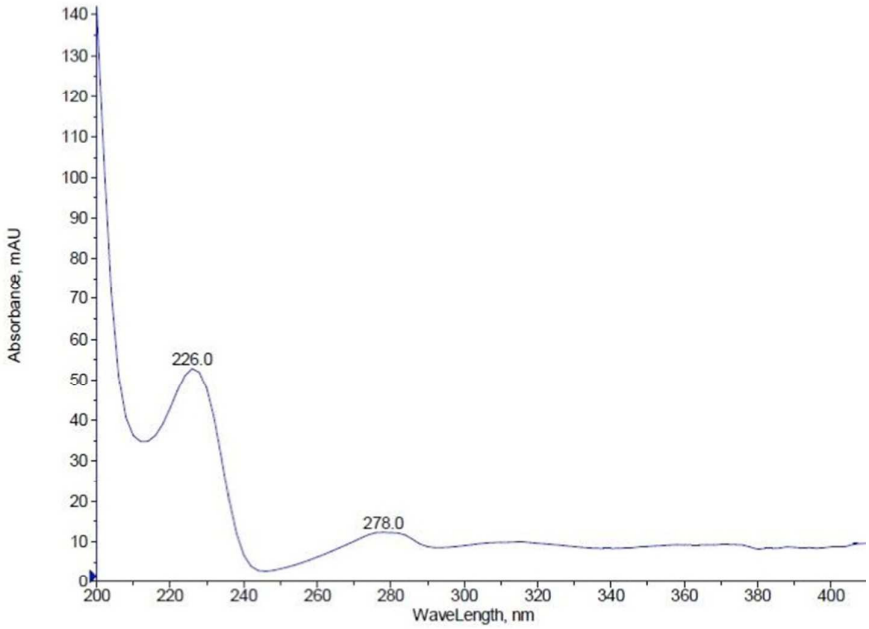

Fig. 2. Absorption spectrum of 50 µg mL^{-1} tirofiban in aqueous solution

Fig. 3 shows LC-MS total and extracted ion chromatograms obtained by analysis of native aqueous solution of tirofiban (50 µg mL^{-1}) and samples submitted to solar irradiated condition. Twelve photoproducts were detected after 6 hours of exposition to simulated sunlight and this outcome accounts for about 15 % *w/w* tirofiban degradation. Even though the degradation process continued beyond to reach 50 % w/w loss of tirofiban after 24h, the photoproducts profile was studied at the early stages of the photodecomposition, not exceeding 15 % *w/w*. Indeed, beyond this level, the likelihood to encounter secondary degradation products is much higher and in such a case, the study may not reflect what would be effectively observed during the in-use conditions. Fig. 4 shows the drug decrease as a function of time, with mention of the photoproducts having appeared during the early stages of the tirofiban photodecomposition.

Thereafter, the photo degradation products are named “PD-n” and numbered according to their elution order (Fig. 3, Fig. 5). Their relative retention times (rRTs) and the HR-MS^n data (origin, exact mass, accurate mass along with relative errors of photoproducts, relevant product ions and number of exchangeable hydrogens) are gathered in Table 1 and the supplementary material.

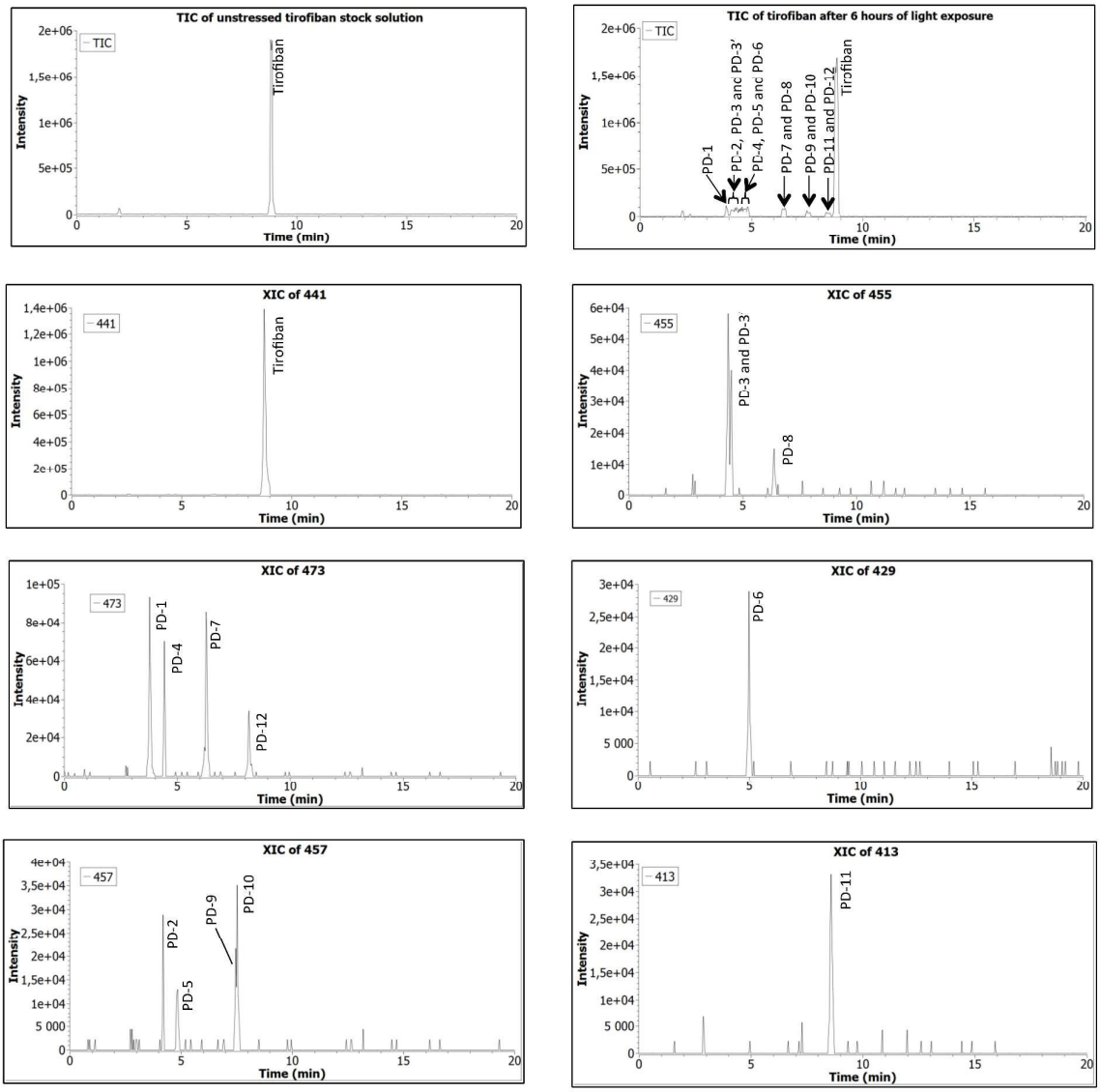

Fig. 3. Total ion chromatograms (TIC) of native and stressed tirofiban aqueous solutions along with extracted ion chromatograms (XIC) of stressed tirofiban after 6 hours of exposure to simulated solar light.

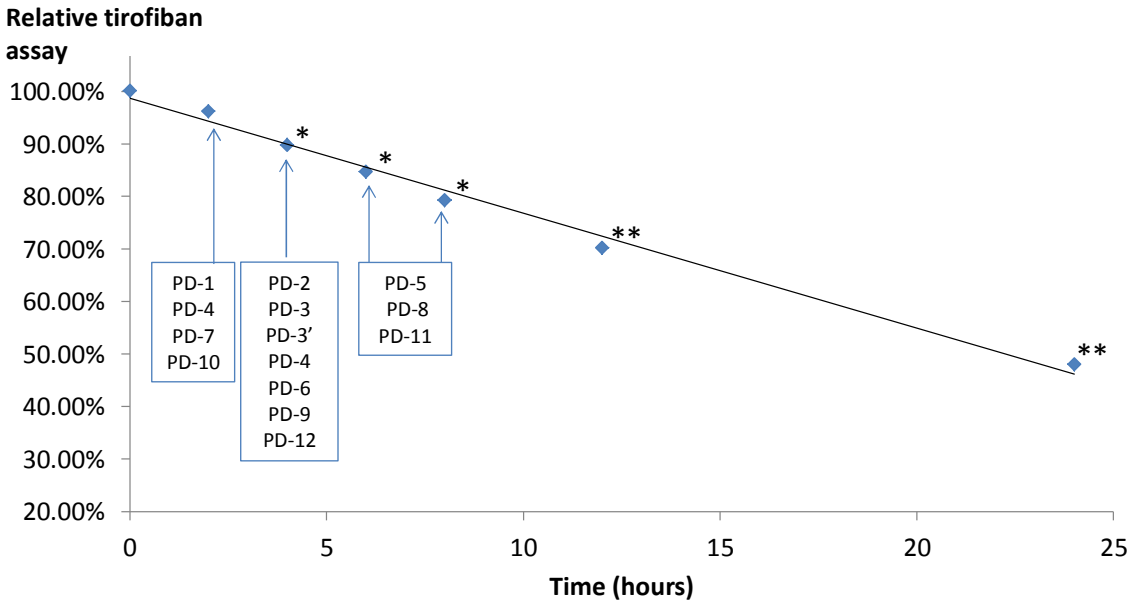

Fig. 4. Relative tirofiban assay as a function of time along with appearance of PDs

* The PDs presented appeared in addition to the previously quoted ones.

** The degradation profile was not investigated at these exposure times.

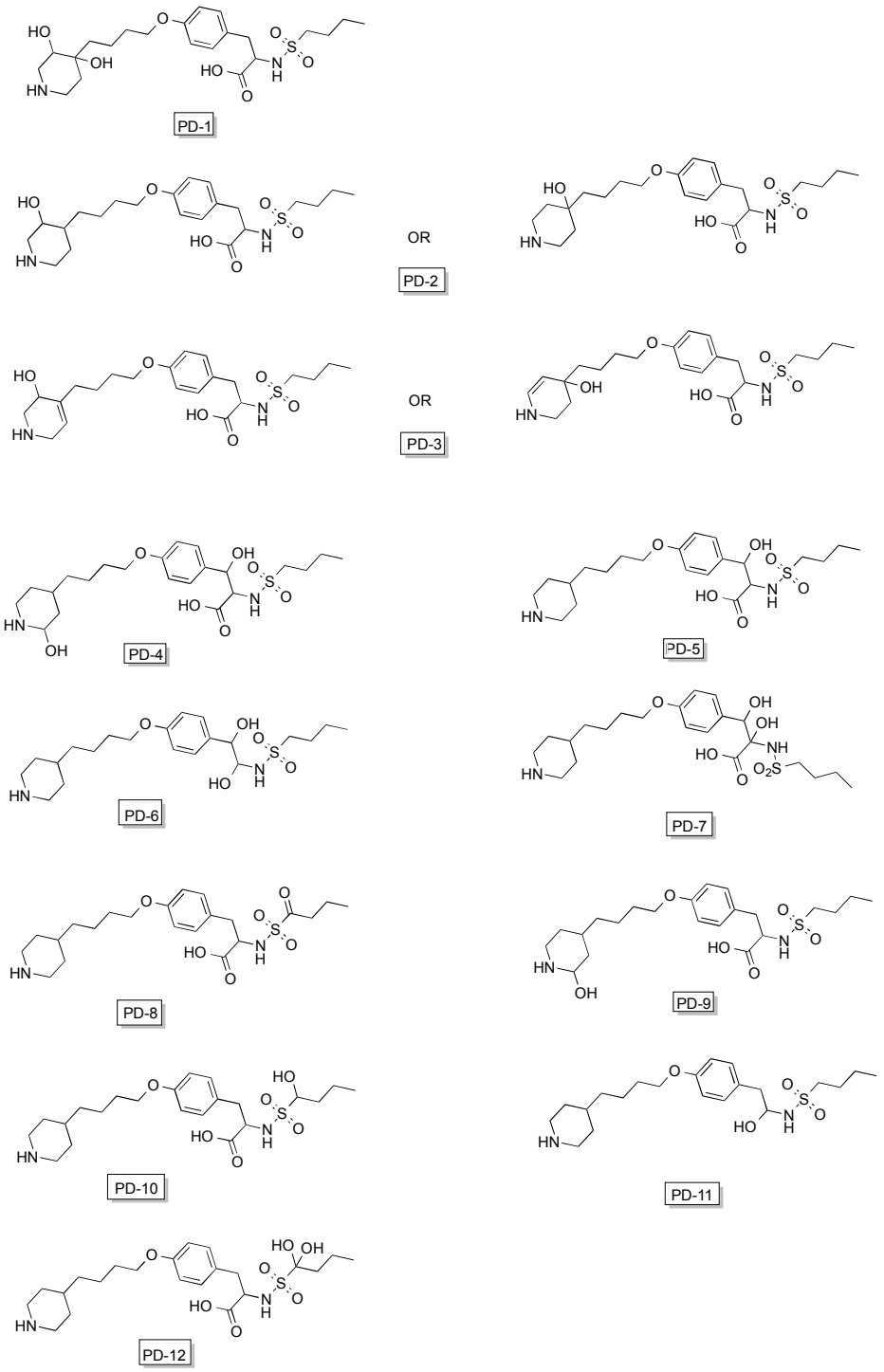

Fig. 5. Structures of the photochemical degradation products detected and characterized in this study.

COMPREHENSIVE STUDY OF TIROFIBAN FRAGMENTATION PATTERN. The fragmentation scheme of tirofiban, which has not been studied in detail so far, was determined using ESI high-resolution multistage mass spectrometry in positive ion mode (ESI^+/HR-MS^n). Analysis was carried out in positive ion mode as it seemed to provide much richer information. Indeed, tirofiban molecule comprises several protonation sites, which may explain its facility to ionize and a rich and complex fragmentation pattern. A thorough understanding of the drug fragmentation pattern is, for a large number of cases, a prerequisite to the degradation products identification. The product ions' structures were systematically confirmed through the elemental composition determination based upon accurate mass measurement. These data are reported in Table 1 and the proposed fragmentation pattern for the drug has been built from multistage ESI^+/HR-MS^n data (Fig. 6 and 7). However, for the sake of homogeneity in terms of graphical representations, the mass-to-charge values linked to each of the structures presented in Figures 7-10, are written in the form of the exact calculated values. Moreover, a structure numbering is done as per an arbitrary mode to facilitate the description of various fragmentation mechanisms (Fig. 7-10).

Table 1. Relative retention times (rRTs), accurate masses with errors, elemental compositions, H/D exchange and MS^n relevant product ions of tirofiban along with photoproducts precursor ions and MS^2 base peaks. Other relevant product ions are provided in supplementary material.

Precursor ion (number of labile hydrogens using H/D exchange)	MSn mode	Best possible elemental formulae	Theoretical mass m/z	Measured Accurate mass m/z	Relative error (ppm)	Relative retention time (Tirofiban's retention time : 8.5 min)
Tirofiban (4)	Precursor ion	$C_{22}H_{37}N_2O_5S^+$	441.24177	441.24073	-2.4	1
	MS^2 (441->)	$C_{21}H_{35}NO_3S^+$	395.23629	395.23542	-2.2	
	MS^2 (441->)	$C_{18}H_{29}N_2O_3^+$	321.21727	321.21668	-1.9	
	MS^2 (441->)	$C_{17}H_{26}NO_2^+$	276.19581	276.19517	-2.3	
	MS^2 (441->)	$C_{17}H_{26}NO^+$	260.20089	260.20026	-2.4	
	MS^2 (441->)	$C_9H_{18}N^+$	140.14338	140.14308	-2.1	
	MS^4 (441->)	$C_8H_{16}N^+$	126.12773	126.12740	-2.6	
	MS^3 (441->395->)	$C_{21}H_{32}N_3OS^+$	378.20974	378.20889	-1.5	
	MS^3 (441->395->)	$C_{17}H_{25}N_2O^+$	273.19614	273.19547	-2.5	
	MS^3 (441->321->)	$C_{17}H_{26}NO_2^+$	276.19581	276.19507	-2.7	
	MS^3 (441->321->)	$C_{17}H_{26}NO^+$	260.20089	260.20016	-2.8	
	MS^3 (441->276->)	$C_{17}H_{24}NO^+$	258.18524	258.18469	-2.1	
	MS^3 (441->276->)	$C_{17}H_{21}O^+$	241.15869	241.15831	-1.6	
	MS^4 (441->321->276->)	$C_9H_{18}N^+$	140.14338	140.14299	-2.8	
	MS^4 (441->321->276->)	$C_8H_{16}N^+$	126.12773	126.12723	-4.0	
	MS^4 (441->321->276->)	$C_6H_{12}N^+$	98.09643	98.09592	-5.2	
	MS^4 (441->395->273->)	$C_{17}H_{22}NO^+$	256.16959	256.16895	-2.5	
	MS^4 (441->395->273->)	$C_{16}H_{22}NO^+$	244.16959	244.16901	-2.4	
	MS^4 (441->395->273->)	$C_9H_{16}N^+$	138.12773	138.12728	-2.9	
	MS^4 (441->395->273->)	$C_8H_{10}NO^+$	136.07569	136.0753	-2.9	
	MS^4 (441->321->260->)	$C_9H_{16}N^+$	138.12773	138.12735	-2.8	
	MS^4 (441->321->260->)	$C_8H_{13}^+$	109.10118	109.10076	-3.8	
	MS^4 (441->321->260->)	$C_5H_8N^+$	82.06513	82.06461	-3.8	
PD-1 (6)	Precursor ion	$C_{22}H_{37}N_2O_7S^+$	473.23160	473.23043	-6.3	0.4
	MS^2 (473->)	$C_{20}H_{31}N_2O_6S^+$	427.18973	427.1887	-2.5	

PD-2 (5)	Precursor ion	$C_{22}H_{37}N_2O_6S^+$	457.23668	457.23549	-2.4	0.48
	MS^2 (457->)	$C_{17}H_{26}NO_3^+$	292.19072	292.18995	-2.6	
PD-3 (5)	Precursor ion	$C_{22}H_{35}N_2O_6S^+$	455.22103	455.21974	-2.6	0.51
	MS^2 (455->)	$C_{22}H_{33}N_2O_5S^+$	437.21047	437.20997	-2.8	
PD-4 (6)	Precursor ion	$C_{22}H_{37}N_2O_7S^+$	473.2316	473.23056	-1.1	0.53
	MS^2 (473->)	$C_{17}H_{25}N_2O_2^+$	289.19105	289.19033	-2.2	
PD-5 (5)	Precursor ion	$C_{22}H_{37}N_2O_6S^+$	457.23668	457.2351	-2.5	0.56
	MS^2 (457->)	$C_{21}H_{35}N_2O_3S^+$	395.23629	395.23517	-3.5	
PD-6 (5)	Precursor ion	$C_{21}H_{37}N_2O_5S^+$	429.24177	429.24093	-2.8	0.59
	MS^2 (429->)	$C_{16}H_{24}NO_2^+$	262.18016	262.17933	-2.0	
PD-7 (6)	Precursor ion	$C_{22}H_{37}N_2O_7S^+$	473.2316	473.23054	-3.2	0.72
	MS^2 (473->)	$C_{21}H_{35}N_2O_3S^+$	395.23629	395.23513	-2.2	
PD-8 (4)	Precursor ion	$C_{22}H_{35}N_2O_6S^+$	455.22103	455.22002	-2.9	0.74
	MS^2 (455->)	$C_{18}H_{29}N_2O_3^+$	321.21727	321.2163	-2.2	
PD-9 (5)	Precursor ion	$C_{22}H_{37}N_2O_6S^+$	457.23668	457.23534	-3.0	0.89
	MS^2 (457->)	$C_{17}H_{24}NO_2^+$	274.18016	274.1797	-2.9	
PD-10 (5)	Precursor ion	$C_{22}H_{37}N_2O_6S^+$	457.23668	457.23504	-1.7	0.9
	MS^2 (457->)	$C_{22}H_{35}N_2O_5S^+$	439.22612	439.22491	-3.6	
PD-11 (4)	Precursor ion	$C_{21}H_{37}N_2O_4S^+$	413.24685	413.24575	-2.8	0.95
	MS^2 (413->)	$C_{17}H_{26}NO_2^+$	276.19581	276.19517	-2.7	
PD-12 (6)	Precursor ion	$C_{22}H_{37}N_2O_7S^+$	473.2316	473.23081	-2.3	0.97
	MS^2 (473->)	$C_{22}H_{35}N_2O_6S^+$	455.22103	455.22041	-1.7	

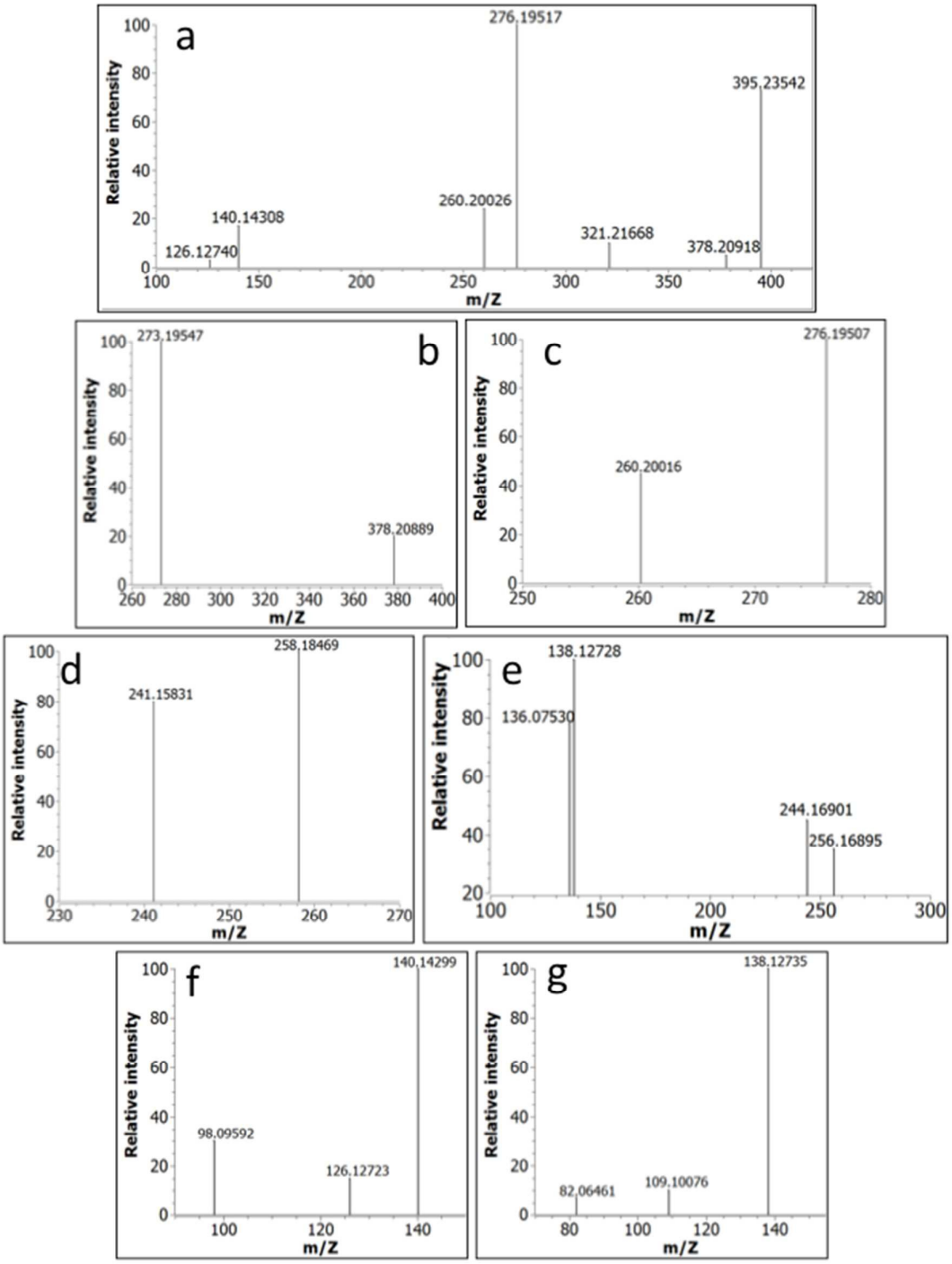

Fig. 6. High-resolution MS^n mass spectra of protonated tirofiban. (a): MS^2 spectrum of protonated tirofiban; (b-d): MS^3 spectra of protonated tirofiban and (b) accounts for 441->395->, (c) for 441->321-> and (d) for 441->276->; (e-g): MS^4 spectra of

protonated tirofiban and (e) accounts for 441->395->273->, (f) for 441->321->273-> and (f) for 441->321->260->.

Tirofiban was detected as protonated $[M+H]^+$ ion (*m/z* 441) and sodium adduct $[M+Na]^+$ ion (*m/z* 463). Its HR-MS^2 spectrum yielded 5 major product ions with *m/z* of 395, 321, 276, 260 and 140 (Fig. 6). The ion of *m/z* 140 seemed to be due to the formation of butylpiperidine carbocation by heterolytic cleavage of O-10'C bond, likely facilitated by O-etheroxide's protonation. The precursor ion could also undergo decarboxylation to afford *m/z* 395 ion, creating a double bond between 2C and 3C. When taken as precursor for MS^3 studies, *m/z* 395 ion yielded *m/z* 273 and *m/z* 378 ions by loss of $C_4H_{10}O_2S$ (-122 Da) and NH_3, respectively. Fragmentation of the most intense MS^3 product ion (*m/z* 273) involved the departure of NH_3 (273➔256) from the piperidine moiety (Fig. 6 and 7). Loss of $C_8H_{17}N$ (-127 Da) was also observed with the formation of *m/z* 146 ion, likely by Mac Lafferty fragmentation. The formation of *m/z* 136 and 138 ions would be the result of an interaction between 2C and 3'C or 5'C, brought near and held close to each other through hydrogen bonds, as shown in Figure 6. A proton transfer from 3'C or 5'C-methylene group towards electron-deficient 2C would have led to the formation of an intermediate of 1N-3'C or 1N-5'C type. A proton transfer from 4'C to 1N would have resulted in the formation of a double bond between 3'C and 4'C (or 5'C and 4'C) and from there, the complementary *m/z* 136 and 138 ions would have been released by O-dealkylation (Fig. 6 and 7). The double bond was unequivocally assigned to 3'C-4'C or 5'C-4'C given the loss of methanal imine (273➔244), occurred by Retro-Diels-Alder fragmentation. In view of such an intra-molecular reactivity, it was critical to thoroughly understanding the different mechanisms involved, in order to avoid

misinterpretation during the identification stage of tirofiban's photoproducts. The formation of *m/z* 276 ion and of *m/z* 260 ion reflected internal migrations of certain chemical groups during the fragmentation process of protonated tirofiban. It was expected that, consecutively to loss of $C_8H_8O_2S$ (-120 Da), affording *m/z* 321 ion, *m/z* 275 ion could easily take over through carboxylic acid elimination. However, the ion at *m/z* 276 turned out to be much more intense. Actually, the premise was that the departure of NH_3 from the ammonium ion (*m/z* 321) would have resulted in a transfer of OH from 1C to $2C^+$ so to fill the electronic gap, thus forming a metastable acylium or oxonium ion, which in turn, would have lost CO to yield *m/z* 276 ion. A similar mechanism could also take place from protonated tirofiban, after elimination of $C_3H_{11}NOS$ and CO (Fig. 7). This assumption was supported by the MS^4 study of *m/z* 276 ion, where a weak dehydration (276➔258) and the formation of the butylpiperidine *m/z* 140 carbocation were highlighted (Fig. 6, Table 1). As *m/z* 276 ion, it was shown that *m/z* 260 ion also stemmed from *m/z* 321 ion (Table 1, Fig. 6 and 7). Its formation mechanism is still not clear but it can be associated to the loss of amino formic acid (-61 Da). A rearrangement mechanism based on 1-6 H-transfer within a six-member centre is proposed. A proton migration from 3'C or the equivalent 5'C toward electron-deficient carbon 2C could have brought about a displacement of NH_2 from 2C to electron-deficient C-carbonyl and the formation of a bond between O-carbonyl and 3'C or 5'C. Ensuing rearrangement would have led to the formation of a derivative whose structure is more suitable to allow the departure of amino formic acid. The structure of *m/z* 260 ion was confirmed by MS^4 studies, showing the presence of *m/z* 138 ion, released by O-dealkylation. The presence of *m/z* 109 ion allowed to confirm the position of the double bond, unequivocally assigned to 3'C-4'C, as shown in Fig. 7.

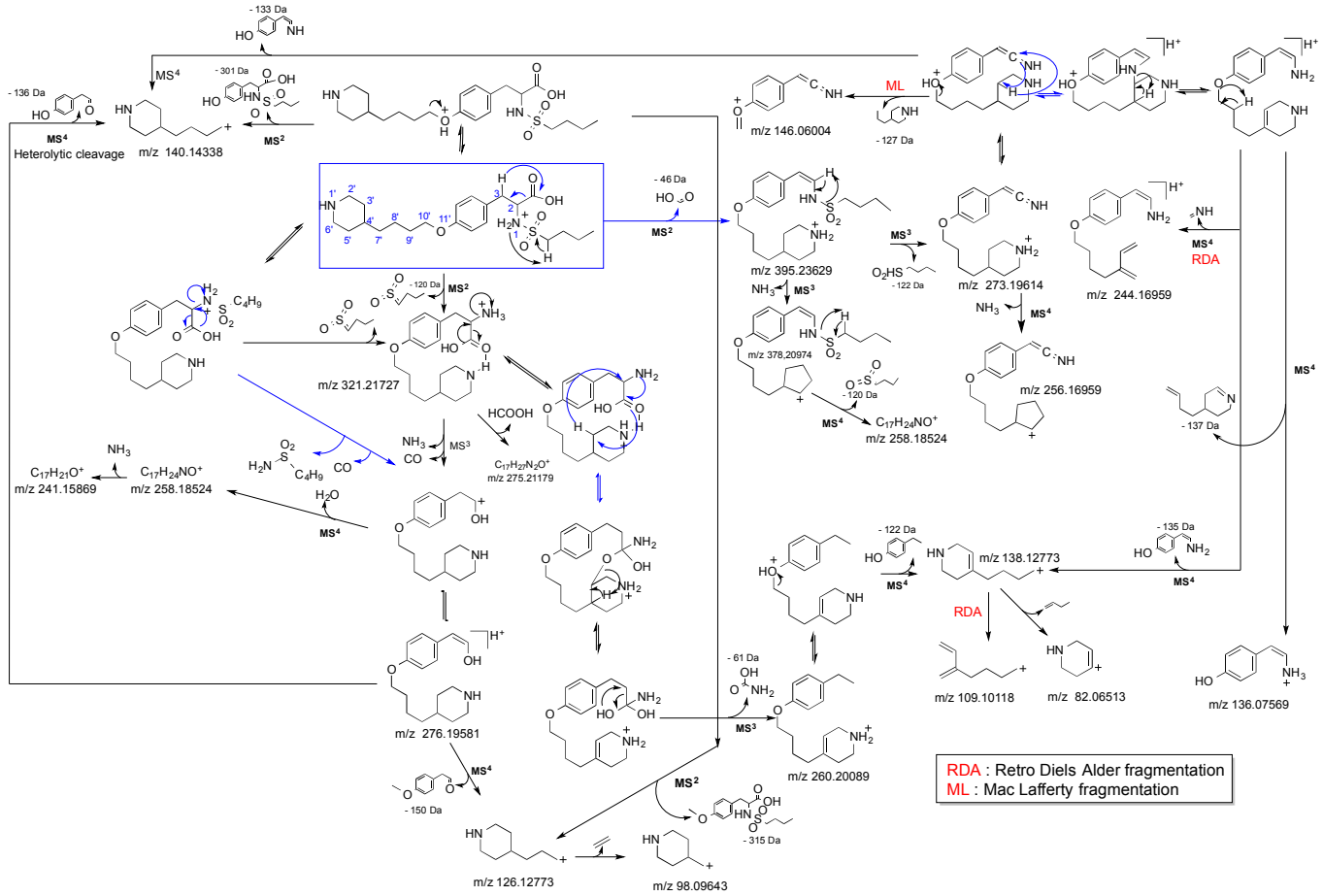

Fig. 7. Fragmentation pattern of protonated tirofiban. Structure numbering was proposed as per an arbitrary mode to facilitate the description of various fragmentation mechanisms.

STRUCTURAL CHARACTERIZATION OF DEGRADATION PRODUCTS. Due to the lack of standards for comparison, identification and elucidation of photoproducts were based on an in-depth analysis of the information gathered from LC-HR-MS^n.

Detected hydroxy-compounds (PD-2, PD-5, PD-9, PD-10 and PD-11). With a mass shift of 16 Da with respect to protonated tirofiban and an accurate mass consistent with elemental composition $C_{22}H_{37}N_2O_6S^+$, PD-2, PD-5, PD-9 and PD-10 are, in all likelihood, tirofiban's OH-derivatives. Since *m/z* 140 ion was clearly detected in the MS^2 spectra of both protonated PD-5 and PD-10, the corresponding segment would have remained identical to that of tirofiban. As all of them underwent dehydration in the course of their fragmentation process, it was possible to rule out the formation of phenolic compounds[19]. On the other side, as protonated PD-2 and PD-9 generated *m/z* 156 ion instead, the presence of an OH-butylpiperidine derivative is to be considered.

More specifically, beyond dehydration, protonated PD-5 could give birth to the benzaldehyde derivative at *m/z* 262, as a result of the losses of $C_4H_8O_2S$, NH_3, CO and methanal as shown in Fig. 8c, while protonated PD-10 was rather characterized by the successive losses of CO (transition 439➔411), NH_3 (transition 411➔394) and of SO_2 (transition 394➔330) after dehydration (Fig. 9). According to the latter case, a six-member ring, involving the carboxyl moiety and the OH function carried by the most stable carbocation of the alkylsulfone group, would have been formed by condensation as shown in Fig. 9. In such a case, the isolated departure of SO_2 without losing the butyl chain can more easily be apprehended. Moreover, the

intense presence of *m/z* 321 ion ([PD-10 + H]$^+$ - $C_4H_8O_3S$) strongly contributed to support the previous assumption. As a result, PD- 5 and PD-10 can be assimilated to N-(butylsulfonyl)-b-hydroxy-O-[4-(piperidin-4-yl)butyl]tyrosine and N-[(1-hydroxybutyl)sulfonyl]-O-[4-(piperidin-4-yl)butyl]tyrosine, respectively. As to PD-2 and PD-9, a simultaneous presence of *m/z* 156 and *m/z* 138 confirmed once more the nature of the product that has been previously postulated. Regarding protonated PD-2, the product ion at *m/z* 393, which was formed by decarboxylation and dehydration, lost methanal imine through Retro-Diels-Alder fragmentation to produce *m/z* 364 ion (Fig. 8a). Therefore, the double bond formed after dehydration can only be located between 3'C and 4'C, suggesting in this, that PD-2 can be assimilated to the 1,3 and/or 1,4 OH-piperidine derivative. Consequently, PD-2 can be assimilated to N-(butylsulfonyl)-O-[4-(3-hydroxypiperidin-4-yl)butyl]tyrosine and/or N-(butylsulfonyl)-O-[4-(4-hydroxypiperidin-4-yl)butyl]tyrosine.

The same approach has also allowed to identify PD-9 as the 1,2 OH-piperidine derivative and/or the N-OH-piperidine derivative. Indeed, instead of forming *m/z* 364 ion, the product ion at *m/z* 393 rather led to that of *m/z* 338 ion by Retro-Diels-Alder fragmentation, thus suggesting that the double bond could only be positioned between 1'N-2'C (Fig. 8b, Table 1 and the supplementary material). Nevertheless, given that the follow-up HDX experiment has shown that the ion at *m/z* 457 increased to *m/z* 462 (Table 1 and the supplementary material), accounting for an exchange of four exchangeable hydrogen and one proton charge, PD-9 can be more precisely identified as N-(butylsulfonyl)-O-[4-(2-hydroxypiperidin-4-yl)butyl]tyrosine.

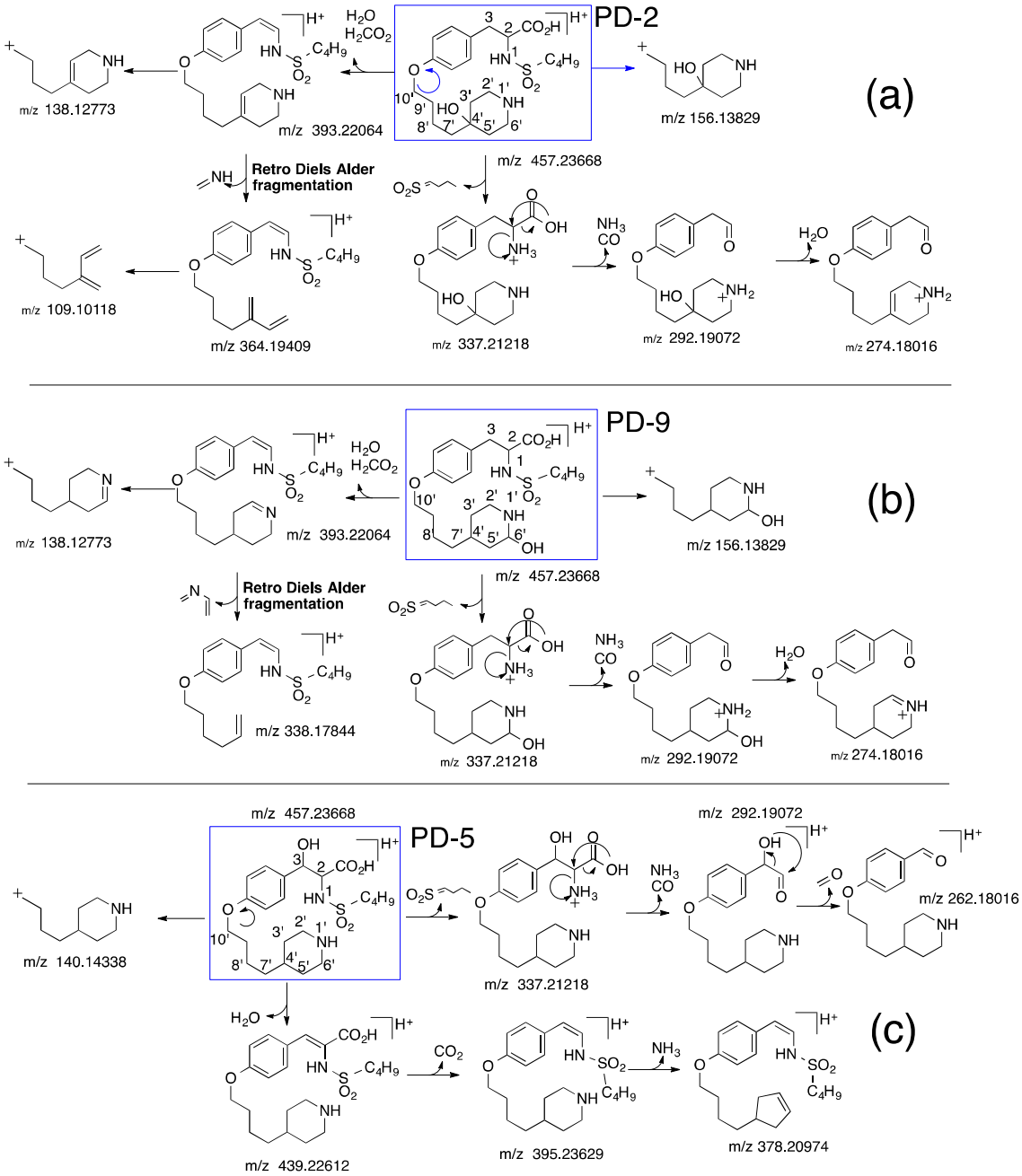

Fig. 8. Fragmentation pathways of protonated PD-2 (a), protonated PD-9 (b) and protonated PD-5 (c).

Based on an accurate mass consistent with elemental composition $C_{21}H_{37}N_2O_4S^+$, PD-11 could be formed by oxidative decarboxylation. Indeed, loss of CO_2 or HCOOH

did not occur when protonated PD-11 was subjected to MS^2 fragmentation (Table 1 and the supplementary material). The *m/z* 395 ion was formed by dehydration so that allows ruling out hydroxylation on the benzyl group. The intense presence of *m/z* 140 and 276 ions has allowed placing the hydroxyl function upon 2C (Fig. 10b). As a result, PD-11 may correspond N-(1-hydroxy-2-{4-[4-(piperidin-4-yl)butoxy]phenyl}ethyl)butane-1-sulfonamide

PD-8 and PD-3. Both protonated PD-3, PD-3' and PD-8 presented a mass shift of 14 Da with respect to that of tirofiban. Their accurate masses were consistent with elemental composition $C_{22}H_{35}N_2O_6S^+$ (Table 1 and the supplementary material). Protonated PD-3 and PD-3', although separated on LC, yielded comparable MS^2 spectra.

The MS^2 spectrum of protonated PD-8 revealed the simultaneous presence of *m/z* 140 and 138 ions, all as protonated tirofiban. The existence of *m/z* 321 ion, which may result from loss of $C_4H_6O_3S$, clearly indicated the presence of a carbonyl function on the carbon chain tied to S-sulfone. Every methylene group can be concerned, but oxidation would more likely occur at the most stable carbocation. 1,6 H-tranfer from 3C to electron-deficient C-carbonyl would have led to the formation of a six-centre ring, whose loss of water would have allowed to directly link 3C to the butyl group as shown in Fig. 9. Next, SO_2 and CO_2 departures occurred to produce *m/z* 373 and 329 ions, respectively. As the fragmentation pattern seems to be in perfect accordance with this assumption (Fig. 9), PD-8 can refer to N-(butanoylsulfonyl)-O-[4-(piperidin-4-yl)butyl]tyrosine.

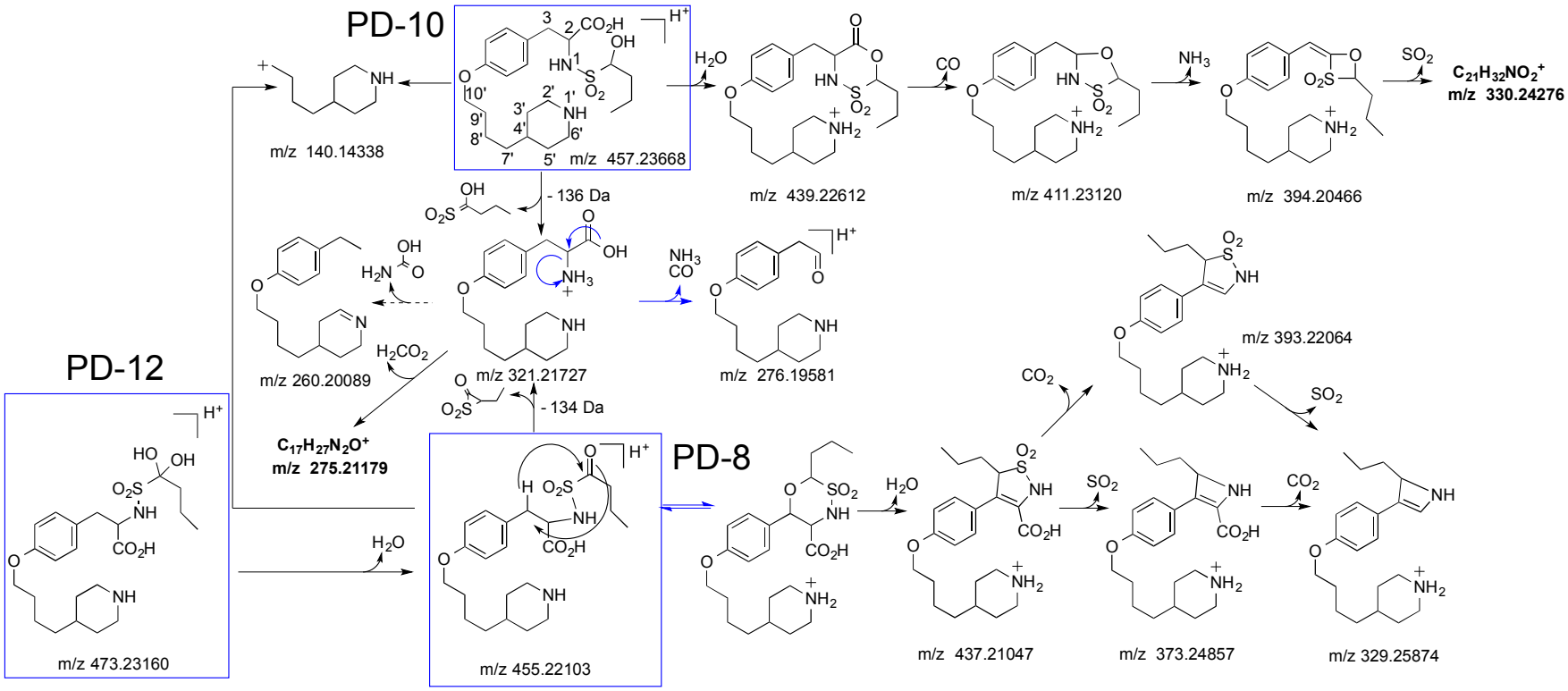

Fig. 9. Fragmentation pathways of protonated PD-8, PD-10 and PD-12.

Unlike protonated PD-8, *m/z* 321 and 140 ions were not detected with protonated PD-3 and PD-3'. Their oxygen-counterparts, detected at *m/z* 335 and 154, respectively, were found instead, suggesting that the butyl piperidine fraction has been altered. Because protonated PD-3/PD-3' and some of their fragments could lose water (455➔437; 154➔136), PD-3/PD-3' cannot be piperidone derivatives. HDX experiments unveiled 5 exchangeable hydrogen, which has allowed to rule out the presence of N-oxide or hydroxylamine functions (Table 1 and the supplementary material). Despite a certain number of structure possibilities and given the analogy that can be done with some other detected photoproducts, PD-3 and PD-3' can account for N-(butylsulfonyl)-O-[4-(4-hydroxy-1,2,3,4-tetrahydropyridin-4-yl)butyl]tyrosine and N-(butylsulfonyl)-O-[4-(3-hydroxy-1,2,3,4-tetrahydropyridin-4-yl)butyl]tyrosine. Nevertheless, those findings need to be confirmed using ^{1}H and ^{13}C-NMR.

Detected diol-compounds (PD-1, PD-4, PD-6, PD-7, and PD-12). With a mass shift of 32 Da with respect to protonated tirofiban and an accurate mass consistent with elemental composition $C_{22}H_{37}N_2O_7S^+$, PD-1, PD-4, PD-7, and PD-12 are in all likelihood tirofiban's diol-derivatives. Their mass spectra were quite different, making them a good basis for identification (Table 1 and the supplementary material).

Taken as precursor for MS^2 studies, protonated PD-7 yielded a certain number of product ions and those with *m/z* of 455, 439, 427, 411, 353, 336, 289, 274, 262 and 140, were the most intense (Table 1 and the supplementary material). The significant presence of *m/z* 140 ion meant that all what pertains to this segment of the starting compound has remained unaltered. Loss of a hydrogen peroxide molecule was

observed (473➔439), suggesting that the two-hydroxyl functions would be in vicinal position and therefore, carried by two adjacent aliphatic carbons. This is in line with the formation of *m/z* 395 ion, by loss of CO_2. The intense formation of *m/z* 262 ion, whose MS^3 studies had allowed to identify it as the benzaldehyde derivative, perfectly corroborates the previous observation (Fig. 10b). Thereof would arise from a rearrangement-cleavage mechanism having led to the departure of a 211 Da moiety corresponding to $C_6H_{13}NO_5S$ as shown in Fig. 10b. Based upon these data, it is safe to identify PD-7 as N-(butylsulfonyl)-a,b-dihydroxy-O-[4-(piperidin-4-yl)butyl]tyrosine.

The MS^2 spectrum of protonated PD-12 featured a great number of common ions with that of PD-8 (Table 1 and the supplementary material, Fig. 9). After dehydration, protonated PD-12 was transformed into protonated PD-8. As a result, PD-12 can be a gem-diol derivative such as N-[(1,1-dihydroxybutyl)sulfonyl]-O-[4-(piperidin-4-yl)butyl]tyrosine.

Unlike the previous case, *m/z* 140 ion was absent from the MS^2 spectrum of protonated PD-1 (Table 1 and the supplementary material, Fig. 10c). Nevertheless, this absence was counterbalanced by the appearance of *m/z* 172 and 138 ions, suggesting that a diOH-butylpiperidine group replaced the butylpiperidine group. Similarly to the previous case, the MS^2 spectrum was marked by an intense presence of *m/z* 439 ion, formed by H_2O_2 loss, which suggested that PD-1 would also be a diol-compound of vicinal type. HDX experiments have highlighted the presence of six exchangeable hydrogens (473➔478), showing that no hydroxylation has occurred upon the secondary amine (Table 1 and the supplementary material). The

ion of *m/z* 364 would have derived from *m/z* 439 ion by successive losses of CO_2 and methanal imine. As previously, a methanal imine loss unequivocally reflected the presence of a double bond between 3'C and 4'C, which has allowed locating the two OH functions. This assumption is in line with an intense loss of ethanol from protonated PD-1, as shown in Fig. 10c. Consequently, PD-1 can be assimilated to N-(butylsulfonyl)-O-[4-(3,4-dihydroxypiperidin-4-yl)butyl]tyrosine.

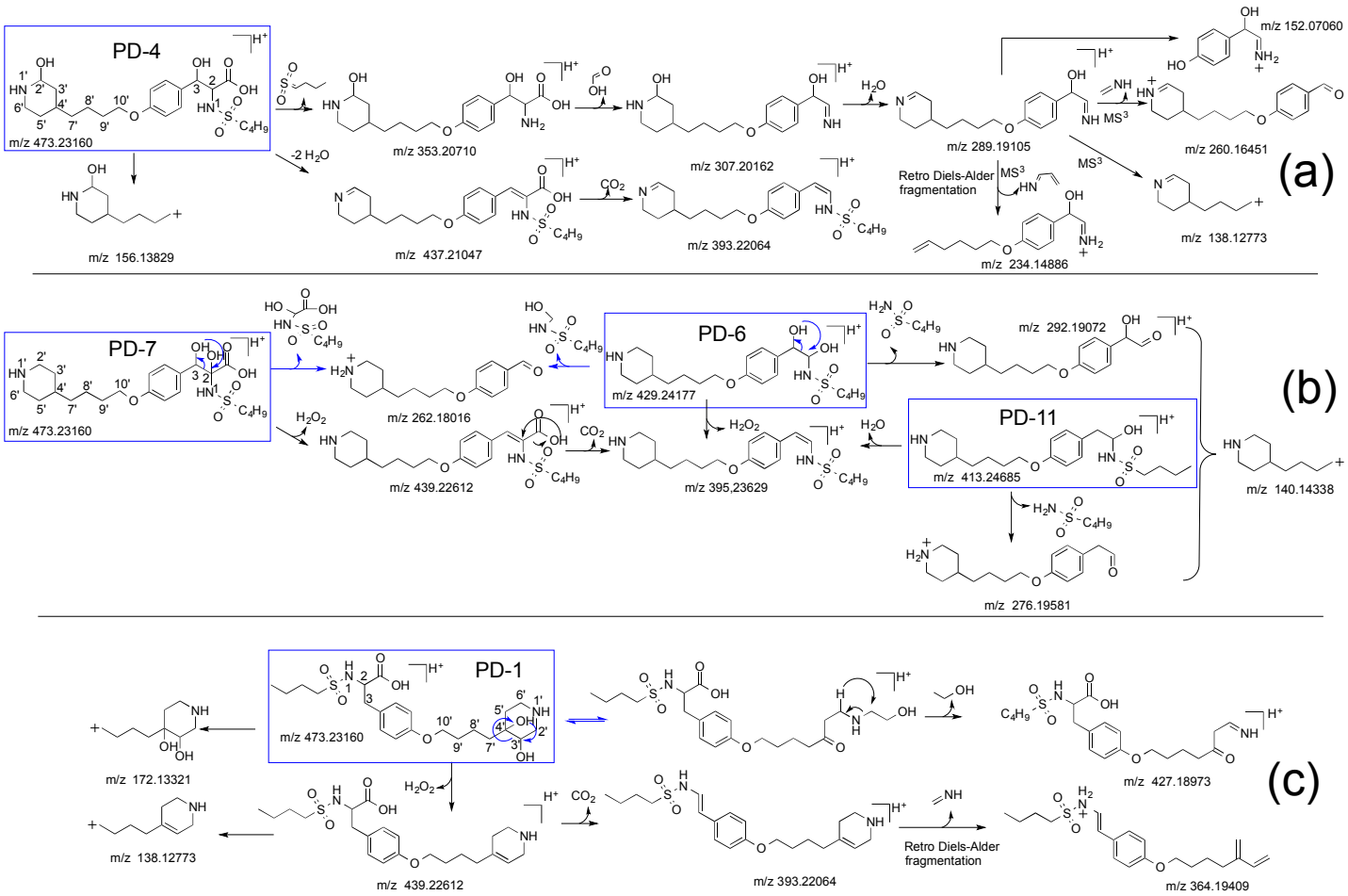

466 **Fig. 10.** Fragmentation pathways of protonated PD-4 (a), PD-6, PD-7 and PD-11 (b) and PD-1 (c).

The MS^2 spectrum of protonated PD-4 has suggested that the two OH functions were located in remote positions, unlike the previous cases. Several elements combined to show that evidence: instead of H_2O_2 loss, a double dehydration occurred (473➔437) and the presence of *m/z* 156 ion demonstrated that the butylpiperidine part only carries one OH function. Taken as precursor for MS^3 studies, the ion at *m/z* 289 ([PD-4 + H - $C_4H_8O_2S$ – H_2CO_2 – $H_2O]^+$) was fragmented as per multiple fragmentation pathways (Fig. 8a), but the two major elements of identification rely on the elimination of C_3H_5N by Retro-Diels-Alder fragmentation (289➔234) and that of methanal imine (289➔260). The first one indicated that an OH function is linked to 2'C or the equivalent 6'C and the other one to 3C. As a result, PD-4 should correspond to N-(butylsulfonyl)-b-hydroxy-O-[4-(2-hydroxypiperidin-4-yl)butyl]tyrosine.

Based upon an accurate mass measurement consistent with elemental composition $C_{21}H_{37}N_2O_5S^+$, PD-6 could be formed by oxidative decarboxylation (Table 1 and the supplementary material). Indeed, loss of CO_2 or H_2CO_2 did not occur when protonated PD-6 was subjected to MS^2 fragmentation (Table 1 and the supplementary material, Fig. 10b). The ion at *m/z* 395 was formed by loss of H_2O_2 and this has allowed to rule out the hypothesis of the benzyl hydroxylation and to opt in favour of the formation of a vicinal-diol compound. The intense presence of *m/z* 140 and 292 ions has allowed assignment of the hydroxyl functions on 2C and 3C. As a result, PD-6 may correspond to N-(1,2-dihydroxy-2-{4-[4-(piperidin-4-yl)butoxy]phenyl}ethyl)butane-1-sulfonamide.

PROPOSED POTENTIAL PHOTO-DEGRADATION PATHWAYS OF TIROFIBAN IN AQUEOUS SOLUTION AND UNDER SUNLIGHT EXPOSURE. Reaching a

certain excited state, tirofiban undergoes autoxidation. The methylene group activated by the aromatic group has been described as being susceptible to auto-oxidation by molecular oxygen[20]. The reaction may be initiated by radical species, abstracting a hydrogen atom from the benzylic carbon atom. The radical then may combine with oxygen to give a hydroperoxy radical. Thereof may abstract a hydrogen atom from any donor present yielding a hydroperoxide, which can degrade by homolytic bond fission to a benzyloxy radical. The abstraction of a hydrogen atom by the hydroperoxide from any donor present results in the benzylic alcohol derivative PD-5. This hydroperoxide can also undergo water elimination to yield the arylketone compound[20], but thereof remained undetected. Even though still not clear, a similar process seems also to occur upon the methylene group activated by the sulphonamide moiety, thus giving rise to the formation of PD-10 and PD-8. PD-12 may be formed by hydration of PD-8 to yield a germinal-diol product[21]. The presence of intermediate peroxides in solution can oxidize the piperidine secondary amine into hydroxylamine piperidine[22], but none of the related products were detected. Oxidation of the piperidine group is still held, but in other parts of the ring. The charge-transfer interaction between excited circulating compounds and the N atom of the secondary amine may be followed by a transfer of α-hydrogen to form a carbon radical intermediate, as shown in Fig. 11. If not immediately reacting with a quencher, one can figure that the hydrogen transfer process can pursue alongside the ring[23]. Radicals 2'C and 4'C can react with soluble O_2, to afford PD-9 and PD-2, after successive rearrangements such as depicted in Fig. 11. PD-4 should have secondarily formed from PD-5 or PD-9 such as proposed in Fig. 11. PD-1 and PD-7 may derive from PD-2 and PD-5, respectively, as per a process successively involving dehydration, epoxide formation and a recombination with water to form a

vicinal-diol compound[24]. As to PD-3 and PD-3', they seem to have derived from PD-1 after dehydration. The methylene group located in β-position with respect to the benzyl group is activated by both an electron-donating (-NH-) and an electron-withdrawing group (-CO_2H). It is then also conducible to autoxidation. But in such a case, a decarboxylation oxidative process should take place as per the captodative effect, responsible for the formation of an oxo-derivative[25]. However, PD-11, which accounts for the hydroxy-decarboxylated compound, was found instead, suggesting that decarboxylation would result from radical $^{\bullet}$OH attack. In the absence of photosensitizers, indirect photolysis through reactions with transients' species should be unexpected or negligible. Therefore, it can be postulated that the presence of $^{\bullet}$OH is probably due to a self-sensitized mechanism under irradiation, but to a lesser extent insofar as hydroxylation on the benzyl ring caused by $^{\bullet}$OH attack[26,27] and O-dealkylation initiated by an attack of this type followed by *ipso* substitution, were not highlighted[28]. In the same way as PD-5/PD-7 or PD-2/PD-1, PD-11 may be an intermediate leading to the formation of PD-6 (Fig. 11).

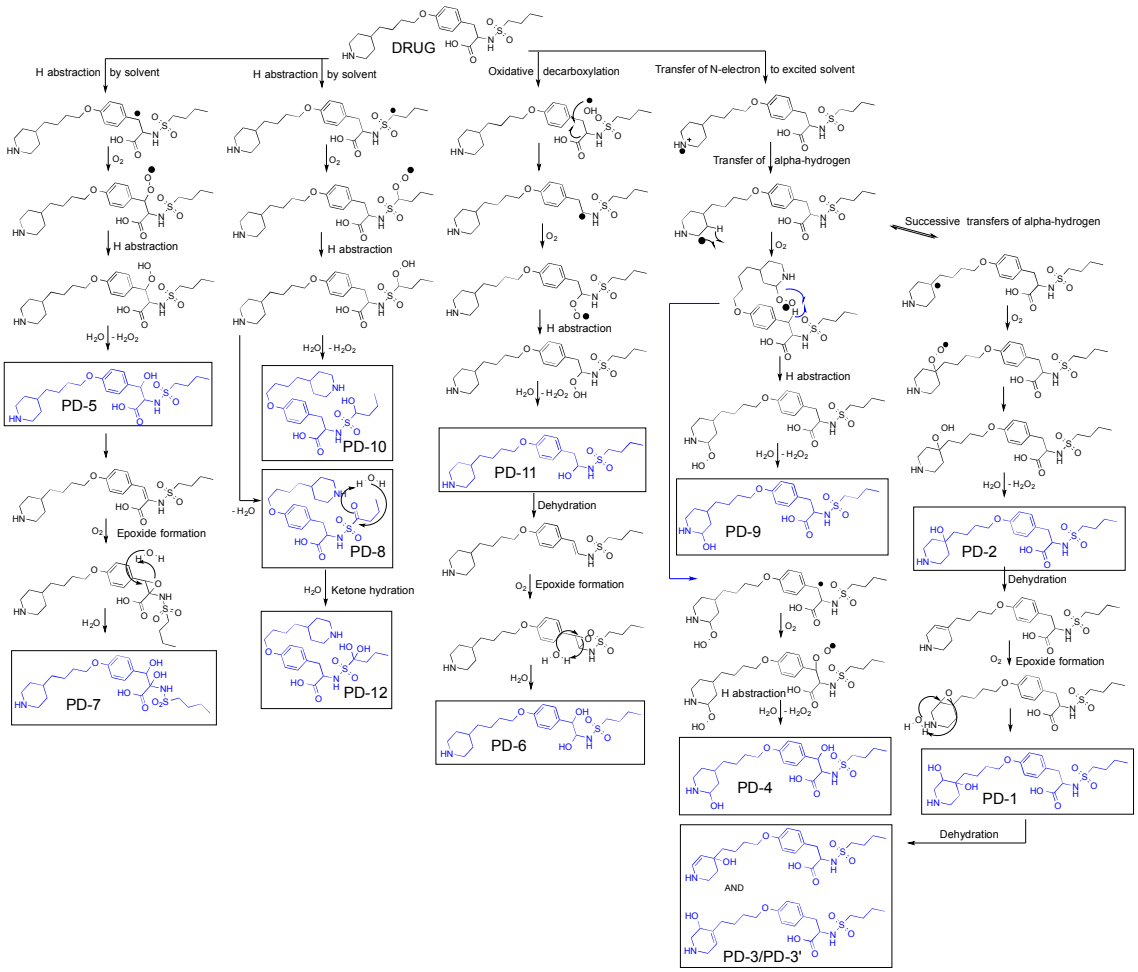

Fig. 11. Photochemical degradation pathways of tirofiban in aqueous solution after irradiation in simulated solar light.

POTENTIAL IMPLICATIONS OF TIROFIBAN PHOTODEGRADATION.

In light of what has been previously found, it appears that tirofiban mostly photodegrades through photosensitized oxidation reactions, rather than through direct photolysis from excited states of the drug. The mechanism proceeds through the transfer of electrons or protons, as previously described, and because oxygen was available in sufficient concentration, molecular oxygen was rapidly added to the radical. In other words, if oxygen was absent or removed, recombination,

dimerization or disproportionation of neutral radicals formed by autoxidation could have occurred. Based upon the UV spectrum of tirofiban, both UV and visible light can induce photosensitized reactions and thus, protection of the active substance against photodegradation during storage/transport/administration can simply consist of preventing the drug product from light exposure, by using, as it is already the case, a secondary opaque packaging. This measure however has a major drawback in that it does not allow visual inspections of the content of the bag before or during the drug infusion. As a result, formulation with good scavengers of free radicals, like glycerol, mannitol and/or ascorbic acid could be a good solution to mitigate photosensitized oxidation reactions in case the drug, despite all, comes to be exposed to light[29].

Photosafety testing is generally considered for pharmaceutical compounds that absorb light between 290 and 700 nm and are applied either topically, or locally, and/or reach the skin or eyes via systemic exposure[30]. Therefore, as far as intravenous tirofiban is concerned, there is no need to include assessments related to photoirritation and photoallergy.

The formation of photoproducts that are, or may be DNA-reactive (genotoxic), can raise concerns if the patient is exposed over a long period. This does not apply to tirofiban since it is used in acute treatment of myocardial infarction. Moreover, the photoproducts formed seem not to be structurally alerting for genotoxicity[31].

▪ CONCLUSION

The data strongly suggest that the photo-transformation of tirofiban in solution can occur via multiple reaction pathways under simulated solar irradiation. The degradation can be initiated by hydrogen abstraction, N-electron extraction or to a

lesser extent, by transient's species attack (•OH), leading to the formation of twelve photo-oxidation products when about 15 % *w/w* degradation of tirofiban was reached. Understanding the main photo-degradation routes is a good basis to work out efficient measures so as to mitigate or avoid instability. Identification of tirofiban's photoproducts can also help assess the potential consequences of the drug photodegradation with respect to the drug potency and safety.

▪ AUTHOR INFORMATION

Corresponding author

*University of Paris-Descartes, Department of Pharmaceutical and Biological Sciences, 4 Avenue de l'Observatoire, 75006 Paris.Email address: bernard.do@parisdescartes.fr. Tel : 33662306275. Fax : 33146691492.

▪ ACKNOWLEDGEMENT

The authors want to thank **K. Manerlax** for her very appreciable contribution to this work. They are also thankful to **Ile de France Region** for financial support in the acquisition of the Orbitrap Velos Pro mass spectrometer

▪ REFERENCES

1 G. D. Hartman, M. S. Egbertson, W. Halczenko, W. L. Laswell, M. E. Duggan, R. L. Smith, A. M. Naylor, P. D. Manno and R.J. Lynch, *J Med Chem*, 1992, **35**,4640-4642.

2 E. J. Topol, T. V. Byzova and E. F. Plow, *The Lancet*, 1999, **353**,227-231.

3 J. G. Xia, Y. Qu, H. Shen and X. H. Liu, *Coron Artery Dis* ,2013, **24**,522-526.

4 T. Huynh, P. Theroux, S. Snapinn and Y. Wan, *Am Heart J*, 2003, **146**,668-673.

5 M.H. Tas, Z. Simsek, A. Ayan, U. Aksu, S. Demirelli, Y. Koza, Z. Lazoglu, B. Seven, H. Senocak , *Adv. Ther*, 2013, **30**, 834-844.

6 I. Mrdovic, L. Savic, R. Lasica, G. Krljanac, M. Asanin, N. Brdar, N. Djuricic, J. Marinkovic and J. Perunicic, *Eur Heart J Acute Cardiovasc Care*, 2014, **3**,56-66.

7 H. De Vries, G. M. J. Beijersbergen van Henegouwen and F.A. Huf, *Int J Pharm*, 1984, **20**,265-271.

8 A. C. Templeton, H. Zu, M. D. Smith, E. Kurali, S. Kleinpeter, K. Jiang and Y. Zhang, *Reg Tox Pharmacol*, 2010, **58**, 224-232.

9 S. Onoue and Y. Tsuda, *Pharm Res*, 2006, **23**, 156-64.

10 A. C. Templeton, H. Xu, J. Placek and R. A. Reed, *Pharm Technol*, 2005, **29**, 68-86.

11 A. M. Lynch, M. D. Smith, A. S. Lane, S. A. Robinson, M. H. Kleinman, S. Kennedy-Gabb, P. Wilcox and R. W. Rees, *Regul Toxicol Pharmacol*, 2010, **58**, 219-23.

12 P.A. Bergquist, D. Manas, W.A. Hunke, R.A. Reed, *Am J Health Syst Pharm*, 2001, **58**, 1218-1223.

13 R. L. Sehgal, *US Pat.* 8,715,920 B2, 2014.

14 M. Narayanam, T. Handa, P. Sharma, S. Jhajra, P. K. Muthe, P. K. Dappili, R.P. Shah and S. Singh, *J Pharm Biomed. Anal*, 2014, **87**,191-211.

15 H. Sadou-Yaye, P. H. Secrétan, T. Henriet, M. Bernard, F. Amrani, W. Akrout, P. Tilleul, N. Yagoubi and B. Do, *J Pharm Biomed Anal*, 2015, **105**, 74-83.

16 F. Amrani, P. H. Secrétan, H. Sadou-Yaye, C. Aymes-Chodur, M. Bernard, A. Solgadi, N. Yagoubi and B. Do, *RSC Adv*, 2015, **5**, 45068-45081.

17 P. H. Secrétan, H. Sadou-Yaye, C. Aymes-Chodur, M. Bernard, A. Solgadi, F. Amrani, N. Yagoubi and B. Do, *RSC Adv*, 2015, **5**, 35586-35597.

18 G. Chen, B. N. Pramanik, Y. H. Liu and U. A. Mirza, *J Mass Spectrom,* 2007, **42**, 279-287.

19 R. Ramanathan, A. D. Su, N. Alvarez, N. Blumenkrantz, S .K. Chowdhury, K. Alton and J. Patrick, *Anal Chem*, 2000, **72**, 1352-1359.

20 S. W. Baertschi and K. M. Alsante, *Pharmaceutical Stress Testing: Prediction Drug degradation*, Taylor and Francis, 2001.

21 E. T. Urbanski, *J Chem Ed*, 2000, **77**, 1644-1647.

22 M. B. Smith and J. March, *March's Advanced Organic Chemistry: Reactions, Mechanisms and Structure*, Wiley-Interscience, 2001.

23 Y. Chen, C. Hu, X. Hu and J. Qu, *Environ Sci Technol*, 2009, **43**, 2760-2765.

24 A. Hartung, M. A. Keane and A. Kraft, *J Org Chem*, 2007, **72**, 10235-10238.

25 H. G. Viehe, Z. Janousek, R. Merenyi and L. Stella, *Acc Chem Res*, 1985, **18**, 148–154.

26 S. Chiron, C. Minero and D. Vione, *Environ Sci Technol*, 2006, **40**, 5977-5983.

27 M. P. Makunina, I. P. Pozdnyakov, Y. Chen, V. P. Grivin, N. M. Bazhin and V. F. Plyusnin, *Chemosphere*, 2015,**119**, 1406-1410.

28 H. Yang, T. An, G. Li, W. Song, W. J. Cooper, H. Luo and X. Guo, *J Hazard Mater*, 2010**, 179**, 834-839.

29 S. Nema and J. D. Ludwig, *Pharmaceutical Dosage Forms: Parenteral Medication*, Informa Healthcare, 2001.

30 International Conferences on Harmonization (ICH) of Technical Requirements for Registration of Pharmaceuticals for Human Use, Topic S10: Photosafety Evaluation of Pharmaceuticals, ICH, Geneva, Switzerland, 2008.

31 D. J. Snodin, *Organic Process Research and Development*, 2010, **14**,960-976.

Phototransformation-Pattern of Antiplatelet Drug Tirofiban in Aqueous Solution, Relevant to Drug Delivery and Storage

Théo Henriet, Philippe-Henry Secrétan, Fatma Amrani, Hassane Sadou-yaye, Mélisande Bernard, Audrey Solgadi, Najet Yagoubi and Bernard Do.

Tirofiban in aqueous solution mostly photodegrades through photosensitized oxidation reactions and the photoproducts formed are not structurally alerting for genotoxicity.